The Dormant Neuron Phenomenon in Deep Reinforcement Learning

Ghada Sokar^{1,2}, Rishabh Agarwal³, Pablo Samuel Castro*³, and Utku Evci*³

¹Eindhoven University of Technology, The Netherlands ²Work done during internship at Google Research ³Google Research

Abstract

In this work we identify the dormant neuron phenomenon in deep reinforcement learning, where an agent's network suffers from an increasing number of inactive neurons, thereby affecting network expressivity. We demonstrate the presence of this phenomenon across a variety of algorithms and environments, and highlight its effect on learning. To address this issue, we propose a simple and effective method (ReDo) that Recycles Dormant neurons throughout training. Our experiments demonstrate that ReDo maintains the expressive power of networks by reducing the number of dormant neurons and results in improved performance.

1 Introduction

The use of deep neural networks as function approximators for value-based reinforcement learning (RL) has been one of the core elements that has enabled scaling RL to complex decision-making problems Bellemare et al. [2020], Mnih et al. [2015], Silver et al. [2016]. However, their use can lead to training difficulties that are not present in traditional RL settings. Numerous improvements have been integrated with RL methods to address training instability, such as the use of target networks, prioritized experience replay, multi-step targets, among others Hessel et al. [2018]. In parallel, there have been recent efforts devoted to better understanding the behavior of neural networks under the learning dynamics of RL Araújo et al. [2021], Bengio et al. [2020], Fu et al. [2019], Kumar et al. [2021a], Lyle et al. [2021], van Hasselt et al. [2018].

Recent work in so-called "scaling laws" for supervised learning problems suggest that, in these settings, there is a positive correlation between performance and the number of parameters Hestness et al. [2017], Kaplan et al. [2020], Zhai et al. [2022]. In RL, however, there is evidence that the networks *lose* their expressivity and ability to fit new targets over time, despite

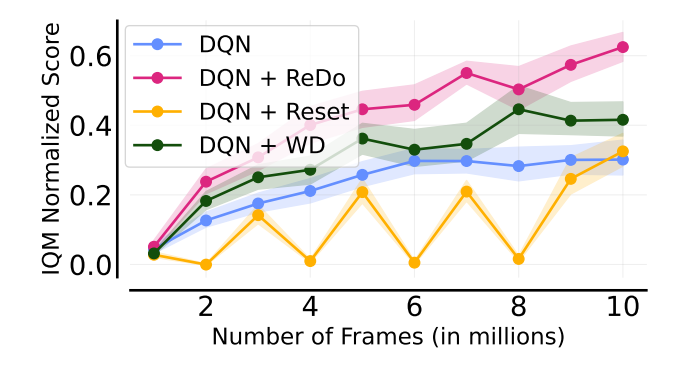


Figure 1: Sample efficiency curves, for DQN with a replay ratio of 1. Additional baselines include Reset [Nikishin et al., 2022] and weight decay (WD). Shaded regions show 95% CIs. The figure shows interquartile mean human-normalized scores, aggregated across 17 Atari games and 5 runs, over the course of training. Among all algorithms, *ReDo* performs the best.

being over-parameterized [Kumar et al., 2021a, Lyle et al., 2021]; this issue has been partly mitigated by perturbing the learned parameters. Igl et al. [2020] and Nikishin et al. [2022] periodically reset some, or all, of the layers of an agent's neural networks, leading to improved performance. These approaches, however, are somewhat drastic: reinitializing the weights can cause the network to "forget" previously learned knowledge and require many gradient updates to recover.

In this work, we seek to understand the underlying reasons behind the loss of expressivity during the training of RL agents. The observed decrease in the learning ability over time raises the following question: Do RL agents use neural network parameters to their full potential? To answer this, we analyze neuron activity throughout training and track dormant neurons: neurons that have become practically inactive through low activations. Our analyses reveal that the number of dormant neurons increases as training progresses, an effect we coin the "dormant neuron phenomenon".

^{*}Equal contribution

Specifically, we find that while agents start the training with a small amount of dormant neurons, this number increases as training progresses. This effect is exacerbated by the number of gradient updates taken per data collection step. This is in contrast with supervised learning, where the number of dormant neurons remains low throughout training.

We demonstrate the presence of the dormant neuron phenomenon across different algorithms and domains: in two value-based algorithms on the Arcade Learning Environment [Bellemare et al., 2013] (DQN Mnih et al. [2015] and $DrQ(\epsilon)$ Agarwal et al. [2021], Yarats et al. [2021]), and with an actor-critic method (SAC Haarnoja et al. [2018]) evaluated on the MuJoCo suite Todorov et al. [2012]. To address this issue, we propose Recycling Dormant neurons (ReDo), a simple and effective method to avoid network under-utilization during training without sacrificing previously learned knowledge: we explicitly limit the spread of dormant neurons by "recycling" them to an active state. ReDo consistently maintains the capacity of the network throughout training and improves the agent's performance (see Figure 1). Our contributions in this work can be summarized as follows:

- We demonstrate the existence of the dormant neuron phenomenon in deep RL.
- We investigate the underlying causes of this phenomenon and show its negative effect on the learning ability of RL agents.
- We propose Recycling Dormant neurons (ReDo), a simple method to reduce the number of dormant neurons and maintain network expressivity during training.
- We demonstrate the effectiveness of ReDo in maximizing network utilization and improving performance.

2 Background

We consider a Markov decision process Puterman [2014], $\mathcal{M} = \langle \mathcal{S}, \mathcal{A}, \mathcal{R}, \mathcal{P}, \gamma \rangle$, defined by a state space \mathcal{S} , an action space \mathcal{A} , a reward function $\mathcal{R}: \mathcal{S} \times \mathcal{A} \to \mathbb{R}$, a transition probability distribution $\mathcal{P}(s'|s,a)$ indicating the probability of transitioning to state s' after taking action a from state s, and a discounting factor $\gamma \in [0,1)$. An agent's behaviour is formalized as a policy $\pi: \mathcal{S} \to Dist(\mathcal{A})$; given any state $s \in \mathcal{S}$ and action $a \in \mathcal{A}$, the value of choosing a from s and following π afterwards is given by $Q^{\pi}(s,a) = \mathbb{E}[\sum_{t=0}^{\infty} \gamma^t \mathcal{R}(s_t,a_t)]$. The goal in RL is to find a policy π^* that maximizes this value: for any π , $Q^{\pi^*} := Q^* \geq Q^{\pi}$.

In deep reinforcement learning, the Q-function is represented using a neural network Q_{θ} with parameters θ . During training, an agent interacts with the environment and collects trajectories of the form $(s, a, r, s') \in \mathcal{S} \times \mathcal{A} \times \mathbb{R} \times \mathcal{S}$. These samples are typically stored in a replay buffer Lin [1992], from which batches are sampled to update the parameters of Q_{θ} using gradient descent. The optimization performed aims to minimize the temporal difference loss Sutton [1988]: $\mathcal{L} = Q_{\theta}(s, a) - Q_{\theta}^{\mathcal{T}}(s, a)$; here, $Q_{\theta}^{\mathcal{T}}(s, a)$ is the bootstrap target $[\mathcal{R}(s, a) + \gamma \max_{a' \in \mathcal{A}} Q_{\tilde{\theta}}(s', a')]$ and $Q_{\tilde{\theta}}$ is a delayed version of Q_{θ} that is known as the target network.

The number of gradient updates performed per environment step is known as the *replay ratio*. This is a key design choice that has a substantial impact on performance Fedus et al. [2020], Kumar et al. [2021b], Nikishin et al. [2022], Van Hasselt et al. [2019]. Increasing the replay ratio can increase the sample-efficiency of RL agents as more parameter updates per sampled trajectory are performed. However, prior works have shown that training agents with a high replay ratio can cause training instabilities, ultimately resulting in decreased agent performance [Nikishin et al., 2022].

One important aspect of reinforcement learning, when contrasted with supervised learning, is that RL agents train on highly non-stationary data, where the non-stationarity is coming in a few forms Igl et al. [2020], but we focus on two of the most salient ones.

Input data non-stationarity: The data the agent trains on is collected in an online manner by interacting with the environment using its current policy π ; this data is then used to update the policy, which affects the distribution of future samples.

Target non-stationarity: The learning target used by RL agents is based on its own estimate $Q_{\tilde{\theta}}$, which is changing as learning progresses.

3 The dormant neuron phenomenon

Prior work has highlighted the fact that networks used in online RL tend to *lose* their expressive ability; in this section we demonstrate that *dormant neurons* play an important role in this finding.

Definition 3.1. Given an input distribution D, let $h_i^{\ell}(x)$ denote the activation of neuron i in layer ℓ under input $x \in D$. We define the score of a neuron i (in layer ℓ) via the normalized average of its activation as follows:

$$s_i^{\ell} = \frac{\mathbb{E}_{x \in D} |h_i^{\ell}(x)|}{\sum_{k \in h} \mathbb{E}_{x \in D} |h_k^{\ell}(x)|}$$
(1)

We say a neuron i in layer ℓ is τ -dormant if $s_i^{\ell} \leq \tau$.

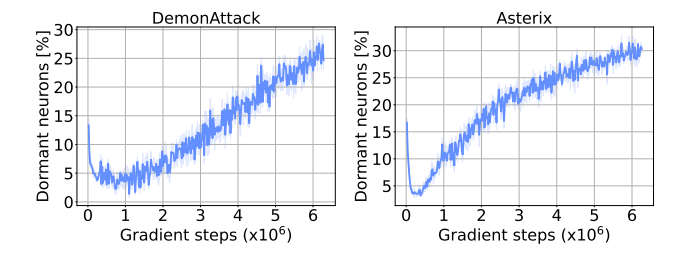


Figure 2: The percentage of dormant neurons increases throughout training for DQN agents.

We normalize the scores such that they sum to 1 within a layer. This makes the comparison of neurons in different layers possible. The threshold τ allows us to detect neurons with low activations. Even though these low activation neurons could, in theory, impact the learned functions when recycled, their impact is expected to be less than the neurons with high activations.

Definition 3.2. An algorithm exhibits the **dormant neuron phenomenon** if the number of τ -dormant neurons in its neural network increases steadily throughout training.

An algorithm exhibiting the dormant neuron phenomenon is not using its network's capacity to its full potential, and this under-utilization worsens over time.

The remainder of this section focuses first on demonstrating that RL agents suffer from the dormant neuron phenomenon, and then on understanding the underlying causes for it. Specifically, we analyze DQN [Mnih et al., 2015, a foundational agent on which most modern value-based agents are based. To do so, we run our evaluations on the Arcade Learning Environment [Bellemare et al., 2013]. For clarity, we focus our analyses on two representative games (DemonAttack and Asterix), but include others in the appendix. In these initial analyses we focus solely on $\tau = 0$ dormancy, but loosen this threshold when benchmarking our algorithm in sections 4 and 5. Additionally, we present analyses on an actor-critic method (SAC Haarnoja et al. [2018]) and a modern sample-efficient agent ($DrQ(\epsilon)$ Yarats et al. [2021]) in Appendix B.

The dormant neuron phenomenon is present in deep RL agents. We begin our analyses by tracking the number of dormant neurons during DQN training. In Figure 2, we observe that the percentage of dormant neurons steadily increases throughout training. This observation is consistent across different algorithms and environments, as can be seen in Appendix B.

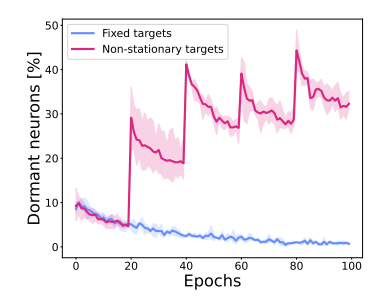


Figure 3: Percentage of dormant neurons when training on CIFAR-10 with fixed and non-stationary targets. Averaged over 3 seeds with shaded areas reporting 95% confidence intervals.

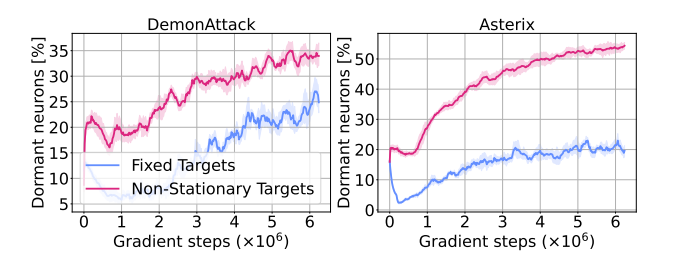
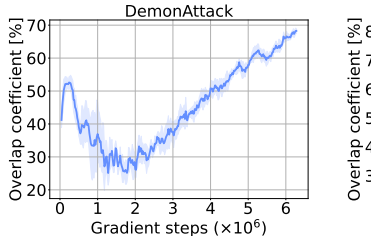


Figure 4: Offline RL. Dormant neurons throughout training with standard moving targets and fixed (random) targets.

Target non-stationarity exacerbates dormant neu-We hypothesize that the non-stationarity of training deep RL agents is one of the causes for the dormant neuron phenomenon. To evaluate this hypothesis, we consider two supervised learning scenarios using the standard CIFAR-10 dataset Krizhevsky et al. [2009]: (1) training a network with fixed targets, and (2) training a network with non-stationary targets, where the labels are shuffled throughout training (see Appendix A for details). As Figure 3 shows, the number of dormant neurons decreases over time with fixed targets. but *increases* over time with non-stationary targets. Indeed, the sharp increases in the figure correspond to the points in training when the labels are shuffled. These findings strongly suggest that the continuously changing targets in deep RL are a significant factor for the presence of the phenomenon.

Input non-stationarity does not appear to be a major factor. To investigate whether the non-stationarity due to online data collection plays a role in exacerbating the phenomenon, we measure the number of dormant neurons in the *offline* RL setting, where an agent is trained on a fixed dataset (we used the dataset



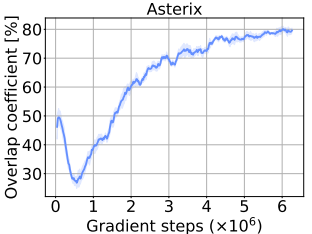
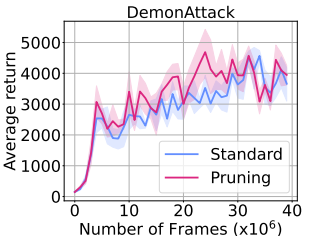


Figure 5: The overlap coefficient of dormant neurons throughout training. There is an increase in the number of dormant neurons that remain dormant.



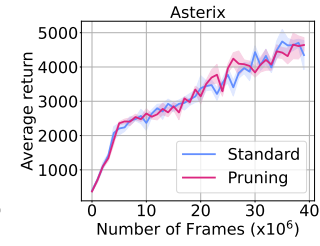
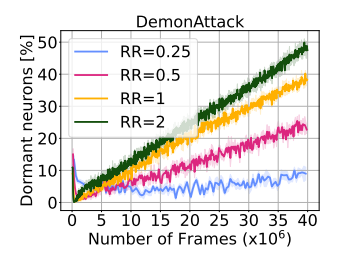


Figure 6: Pruning dormant neurons during training does not affect the performance of an agent.

provided by Agarwal et al. [2020]). In Figure 4 we can see that the phenomenon remains in this setting, suggesting that input non-stationary is not one of the primary contributing factors. To further analyze the source of dormant neurons in this setting, we train RL agents with *fixed* random targets (ablating the non-stationarity in inputs and targets). The decrease in the number of dormant neurons observed in this case (Figure 4) supports our hypothesis that the moving targets in RL training are the primary source of this phenomenon.

Dormant neurons remain dormant. To investigate whether dormant neurons "reactivate" as training progresses, we track the overlap in the set of dormant neurons. Figure 5 plots the overlap coefficient between the set of dormant neurons in the penultimate layer at the current iteration, and the historical set of dormant neurons.* The increase shown in the figure strongly suggests that once a neuron becomes dormant, it remains that way for the rest of training. To further investigate this, we explicitly *prune* any neuron found dormant throughout training, to check whether their removal affects the agent's overall performance. As Fig-



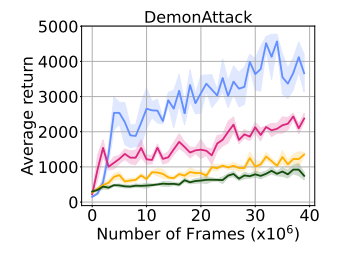


Figure 7: The rate of increase in dormant neurons with varying replay ratio (RR) (left). The higher percentage of dormant neurons correlates with the performance drop that occurs when the replay ratio is increased (right).

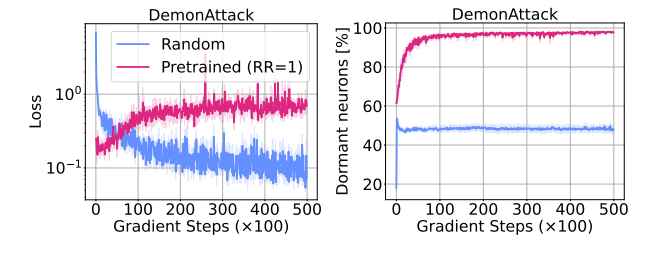


Figure 8: A pretrained network that exhibits dormant neurons has less ability than a randomly initialized network to fit a fixed target. Results are averaged over 5 seeds.

ure 6 shows, their removal does not affect the agent's performance, further confirming that dormant neurons remain dormant.

More gradient updates leads to more dormant neurons. Although an increase in replay ratio can seem appealing from a data-efficiency point of view (as more gradient updates per environment step are taken), it has been shown to cause overfitting and performance collapse Kumar et al. [2021a], Nikishin et al. [2022]. In Figure 7 we measure neuron dormancy while varying the replay ratio, and observe a strong correlation between replay ratio and the fraction of neurons turning dormant. Although difficult to assert conclusively, this finding could account for the difficulty in training RL agents with higher replay ratios; indeed, we will demonstrate in Section 5 that recycling dormant neurons and activating them can mitigate this instability, leading to better results.

Dormant neurons make learning new tasks more difficult. We directly examine the effect of dormant neurons on an RL network's ability to learn new tasks. To do so, we train a DQN agent with a replay ratio of 1

^{*}The overlap coefficient between two sets X and Y is defined as $overlap(X,Y) = \frac{|X \cap Y|}{\min(|X|,|Y|)}$.

(this agent exhibits a high level of dormant neurons as observed in Figure 7). Next we fine-tune this network by distilling it towards a well performing DQN agent's network, using a traditional regression loss and compare this with a randomly initialized agent trained using the same loss. In Figure 8 we see that the pre-trained network, which starts with a high level of dormant neurons, shows degrading performance throughout training; in contrast, the randomly initialized baseline is able to continuously improve. Further, while the baseline network maintains a stable level of dormant neurons, the number of dormant neurons in the pre-trained network continues to increase throughout training.

4 Recycling Dormant neurons (ReDo)

Our analyses in Section 3, which demonstrates the existence of the dormant neuron phenomenon in online RL, suggests these dormant neurons may have a role to play in the diminished expressivity highlighted by Kumar et al. [2021a] and Lyle et al. [2021]. To account for this, we propose to **re**cycle **dormant** neurons periodically during training (ReDo).

The main idea of ReDo, outlined in Algorithm 1, is rather simple: during regular training, periodically check whether any neurons are τ -dormant; for these, reinitialize their incoming weights and zero out the outgoing weights. The incoming weights are initialized using the original weight distribution. Note that if τ is 0, we are effectively leaving the network's output unchanged; if τ is small, the output of the network is only slightly changed.

Figure 9 showcases the effectiveness of ReDo in dramatically reducing the number of dormant neurons, which also results in improved agent performance. Before diving into a deeper empirical evaluation of our method in Section 5, we discuss some algorithmic alternatives we considered when designing ReDo.

Alternate recycling strategies. We considered other recycling strategies, such as scaling the incoming connections using the mean of the norm of non-dormant neurons. However, this strategy performed similarly to using initial weight distribution. Similarly, alternative initialization strategies like initializing outgoing connections randomly resulted in similar or worse returns. Results of these investigations are shared in Appendix C.2.

Are ReLUs to blame? RL networks typically use ReLU activations, which can saturate at zero outputs, and hence zero gradients. To investigate whether the issue is specific to the use of ReLUs, in Appendix C.1 we measured the number of dormant neurons and resulting performance when using a different activation function. We observed that there is a mild decrease in

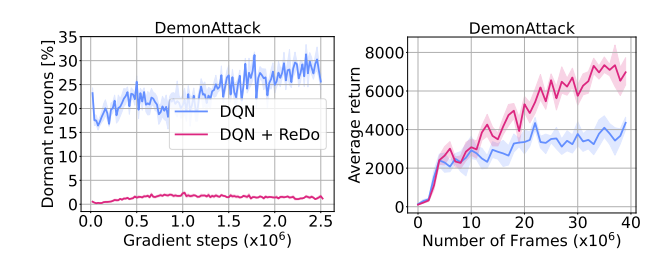


Figure 9: Evaluation of ReDo's effectiveness (with $\tau = 0.025$) in reducing dormant neurons (left) and improving performance (right) on DQN.

Algorithm 1 ReDo

Input: Network parameters θ , threshold τ , training steps T, frequency F for t=1 to to T do

Update θ with regular RL loss if $t \mod F == 0$ then for each neuron i do

if $s_i^\ell \leq \tau$ then

Reinitialize input weights of neuron iSet outgoing weights of neuron i to 0end if end for end for

the number of dormant neurons, but the phenomenon is still present.

5 Empirical evaluations

Agents, architectures, and environments. We evaluate DQN on 17 games from the Arcade Learning Environment [Bellemare et al., 2013] (as used in Kumar et al. [2021a,b] to study the loss of network expressivity). We study two different architectures: the default CNN used by Mnih et al. [2015], and the ResNet architecture used by the IMPALA agent [Espeholt et al., 2018].

Additionally, we evaluate $DrQ(\epsilon)$ Agarwal et al. [2021], Yarats et al. [2021] on the 26 games used in the Atari 100K benchmark [Kaiser et al., 2019], and SAC [Haarnoja et al., 2018] on MuJoCo environments [Todorov et al., 2012].

Implementation details. All our experiments and implementations were conducted using the Dopamine framework [Castro et al., 2018]*. For agents trained with ReDo, we use a threshold of $\tau = 0.1$, unless otherwise noted, as we found this gave a better performance

^{*}Code is available at https://github.com/google/dopamine/tree/master/dopamine/labs/redo

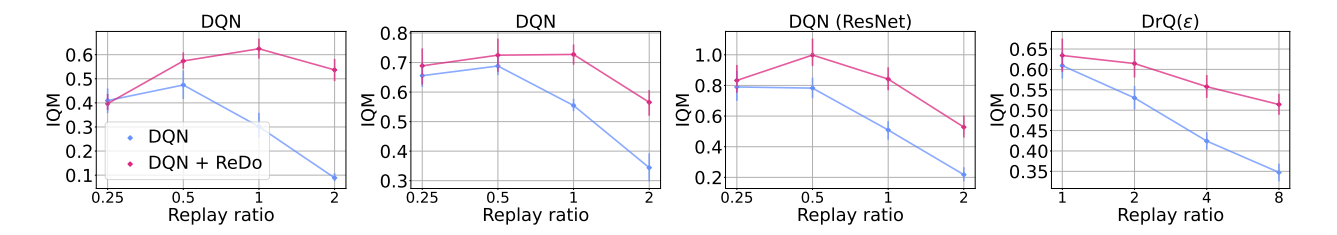


Figure 10: Evaluating the effect of increased replay ratio with and without ReDo. From left to right: DQN with default settings, DQN with n-step of 3, DQN with the ResNet architecture, and $DrQ(\epsilon)$. We report results using 5 seeds, while $DrQ(\epsilon)$ use 10 seeds; error bars report 95% confidence intervals.

than using a threshold of 0 or 0.025. When aggregating results across multiple games, we report the Interquantile Mean (IQM), recommended by Agarwal et al. [2021] as a more statistically reliable alternative to median or mean, using 5 independent seeds for each DQN experiment, 10 for the DrQ and SAC experiments, and reporting 95% stratified bootstrap confidence intervals.

5.1 Consequences for sample efficiency

Motivated by our finding that higher replay ratios exacerbate dormant neurons and lead to poor performance (Figure 7), we investigate whether ReDo can help mitigate these. To do so, we report the IQM for four replay ratio values: 0.25 (default for DQN), 0.5, 1, and 2 when training with and without ReDo. Since increasing the replay ratio increases the training time and cost, we train DQN for 10M frames, as opposed to the regular 200M. As the leftmost plot in Figure 10 demonstrates, ReDo is able to avoid the performance collapse when increasing replay ratios, and even to benefit from the higher replay ratios when trained with ReDo.

Impact on multi-step learning. In the center-left plot of Figure 10 we added n-step returns with a value of n=3 [Sutton and Barto, 2018]. While this change results in a general improvement in DQN's performance, it still suffers from performance collapse with higher replay ratios; ReDo mitigates this and improves performance across all values.

Varying architectures. To evaluate ReDo's impact on different network architectures, in the centerright plot of Figure 10 we replace the default CNN architecture used by DQN with the ResNet architecture used by the IMPALA agent Espeholt et al. [2018]. We see a similar trend: ReDo enables the agent to make better use of higher replay ratios, resulting in improved performance.

Varying agents. We evaluate on a sample-efficient value-based agent $DrQ(\epsilon)$ Agarwal et al. [2021], Yarats et al. [2021]) in the rightmost plot of Figure 10. In this setting, we train for 400K steps, where we can

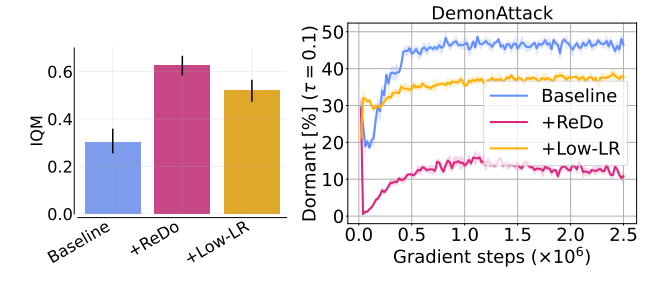


Figure 11: Effect of reduced learning rate in high replay ratio setting. Scaling learning rate helps, but does not solve the dormant neuron problem.

see the effect of dormant neurons on performance, and study the following replay ratio values: 1 (default), 2, 4, 8. Once again, we observe ReDo's effectiveness in improving performance at higher replay ratios.

In the rest of this section, we do further analyses to understand the improved performance of ReDo and how it fares against related methods. We perform this study on a DQN agent trained with a replay ratio of 1.

5.2 Learning rate scaling

An important point to consider is that the default learning rate may not be optimal for higher replay ratios. Intuitively, performing more gradient updates would suggest a reduced learning rate would be more beneficial. To evaluate this, since we are using a replay ratio of 1 (four times the default value), we decrease the learning rate by a factor of four. Figure 11 confirms that a lower learning rate reduces the number of dormant neurons and improves performance. Interestingly, using ReDo with a high replay ratio and the default learning rate obtains the best performance. This result suggests ReDo can facilitate increasing sample efficiency, as it may require less hyper-parameter optimization.

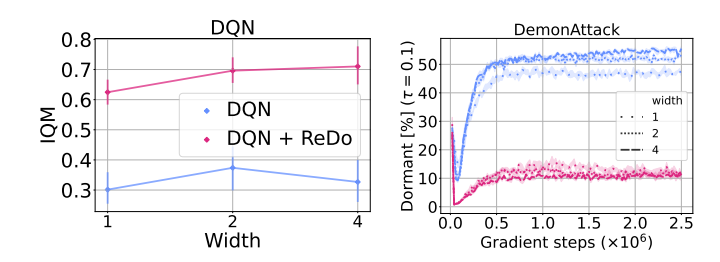


Figure 12: Performance of DQN trained with RR=1 using different network width. Increasing the width of the network slightly improves the performance. Yet, the performance gain does not reach the gain obtained by ReDo. ReDo improves the performance across different network sizes.

5.3 Is over-parameterization enough?

Lyle et al. [2021] and Fu et al. [2019] suggest sufficiently over-parameterized networks can fit new targets over time; this raises the question of whether over-parameterization can help address the dormant neuron phenomenon. To investigate this, we increase the size of the DQN network by doubling and quadrupling the width of its layers (both the convolutional and fully connected). The left plot in Figure 12 shows that larger networks have at most a mild positive effect on the performance of DQN, and the resulting performance is still far inferior to that obtained when using ReDo with the default width. Furthermore, training with ReDo seems to improve as the network size increases, suggesting that the agent is able to better exploit network parameters, compared to when training without ReDo.

An interesting finding in the right plot in Figure 12 is that the percentage of dormant neurons is similar across the varying widths. As expected, the use of ReDo dramatically reduces this number for all values. This finding is somewhat at odds with that from Sankararaman et al. [2020]. They demonstrated that, in supervised learning settings, increasing the width decreases the gradient confusion and leads to faster training. If this observation would also hold in RL, we would expect to see the percentage of dormant neurons decrease in larger models.

5.4 Comparison with related methods

Nikishin et al. [2022] also observed performance collapse when increasing the replay ratio, but attributed this to overfitting to early samples (an effect they refer to as the "primacy bias"). To mitigate this, they proposed periodically resetting the network, which can be seen as a form of regularization. We compare the perfor-

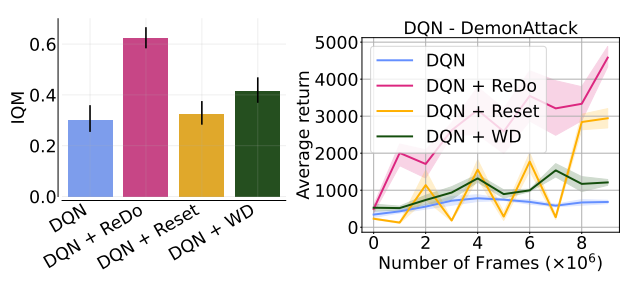


Figure 13: Comparison of the performance for *ReDo* and two different regularization methods (Reset and WD) when integrated with training DQN agents.

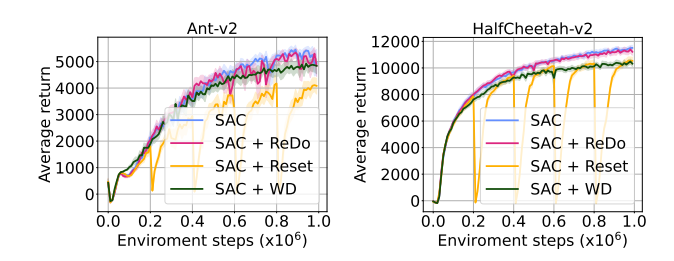


Figure 14: Comparison of the performance of SAC agents with *ReDo* and two different regularization methods. See Figure 20 for other environments.

mance of ReDo against theirs, which periodically resets only the penultimate layer for Atari 2600 environments. Additionally, we compare to adding weight decay, as this is a simpler, but related, form of regularization. It is worth highlighting that Nikishin et al. [2022] also found high values of replay ratio to be more amenable to their method. As Figure 13 illustrates, weight decay is comparable to periodic resets, but ReDo is superior to both.

We continue our comparison with resets and weight decay on two MuJoCo environments with the SAC agent [Haarnoja et al., 2018]. As Figure 14 shows, ReDo is the only method that does not suffer a performance degradation.

5.5 Neuron selection strategies

Finally, we compare our strategy for selecting the neurons that will be recycled (section 3) against two alternatives: (1) **Random:** neurons are selected randomly, and (2) **Inverse ReDo:** neurons with the *highest* scores according to Equation 1 are selected. To ensure a fair comparison, the number of recycled neurons is a fixed percentage for all methods, occurring every 1000 steps. The percentage of neurons to recycle follows a cosine schedule starting at 0.1 and ending at 0. As Figure 15 shows, recycling active or random neurons

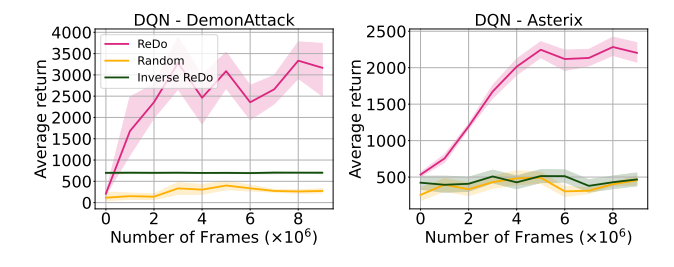


Figure 15: Comparison of different strategies for selecting the neurons that will be recycled.

hinders learning and causes performance collapse.

6 Related Work

Function approximators in RL The use of overparameterized neural networks as function approximators was instrumental to some of the successes in RL, such as achieving superhuman performance on Atari 2600 games Mnih et al. [2015] and continuous control Lillicrap et al. [2016]. Recent works observe a change in the network's capacity over the course of training, which affects the agent's performance. Kumar et al. [2021a,b] show that the expressivity of the network decreases gradually due to bootstrapping. Gulcehre et al. [2022] investigate the sources of expressivity loss in offline RL and observe that underparamterization emerges with prolonged training. Lyle et al. [2021] demonstrate that RL agents lose their ability to fit new target functions over time, due to the non-stationary in the targets. Similar observations have been found, referred to as plasticity loss, in the continual learning setting where the data distribution is changing over time Berariu et al. [2021], Dohare et al. [2021]. These observations call for better understanding how RL learning dynamics affect the capacity of their neural networks.

There is a recent line of work investigating network topologies by using sparse neural networks in online Graesser et al. [2022], Sokar et al. [2022], Tan et al. [2022] and offline RL Arnob et al. [2021]. They show up to 90% of the network's weights can be removed with minimal loss in performance. This suggests that RL agents are not using the capacity of the network to its full potential.

Generalization in RL RL agents are prone to overfitting, whether it is to training environments, reducing their ability to generalize to unseen environments Kirk et al. [2021], or to early training samples, which degrades later training performance Fu et al. [2019], Nikishin et al. [2022]. Techniques such as regularization Hiraoka et al. [2021], Wang et al. [2020], ensembles Chen et al. [2020], or data augmentation Fan et al. [2021], Hansen et al. [2021], Janner et al. [2019] have been adopted to account for overfitting.

Another related line of work re-initializes a subset or all of the weights of a neural network during training. This technique is mainly explored in supervised learning Alabdulmohsin et al. [2021], Taha et al. [2021], Zaidi et al. [2022], Zhou et al. [2021], transfer learning Li et al. [2020], and online learning Ash and Adams [2020]. A few recent works have explored this for RL: Igl et al. [2020] periodically reset an agent's full network and then performs distillation from the prereset network. Nikishin et al. [2022] (already discussed in Figure 13) periodically resets the last layers of an agent's network. Despite its performance gains, fully resetting some or all layers can lead to the agent "forgetting" prior learned knowledge. The authors account for this by using a sufficiently large replay buffer, so as to never discard any observed experience; this, however, makes it difficult to scale to environments with more environment interactions. Further, recovering performance after each reset requires many gradient updates. Similar to our approach, Dohare et al. [2021] adapt the stochastic gradient descent by resetting the smallest utility features for continual learning. We compare their utility metric to the one used by ReDo in Appendix C.4 and observe similar or worse performance. Neural network growing A related research direction is to prune and grow the architecture of a neural network. On the growing front, Evci et al. [2021] and Dai et al. [2019] proposed gradient-based strategies to grow new neurons in dense and sparse networks, respectively. Yoon et al. [2018] and Wu et al. [2019] proposed methods to split existing neurons. Zhou et al. [2012] adds new neurons and merges similar features for online learning.

7 Discussion and Conclusion

In this work we identified the dormant neuron phenomenon, whereby, during training, an RL agent's neural network exhibits an increase in the number of neurons with little-or-no activation. We demonstrated that this phenomenon is present across a variety of algorithms and domains, and provided evidence that it does result in reduced expressivity and inability to adapt to new tasks. To overcome this issue, we proposed a simple method to maintain network utilization throughout training by periodic recycling of dormant neurons.

The simplicity of ReDo allows for easy integration with existing RL algorithms. Our experiments suggest

that this can lead to improved performance. Indeed, the results in Figure 10 and 12 suggest that ReDo can be an important component in being able to successfully scale RL networks in a sample-efficient manner. Although the simple approach of recycling neurons we introduced yielded good results, it is possible that better approaches exist. For example, ReDO reduces dormant neurons significantly but it doesn't completely eliminate them. Further research on initialization and optimization of the recycled capacity can address this and lead to improved performance.

Interestingly, studies in neuroscience have found similar types of dormant neurons (precursors) in the adult brain of several mammalian species, including humans Benedetti and Couillard-Despres [2022], albeit with different dynamics. Certain brain neurons start off as dormant during embryonic development, and progressively awaken with age, eventually becoming mature and functionally integrated as excitatory neurons Benedetti and Couillard-Despres [2022], Benedetti et al. [2020], Rotheneichner et al. [2018]. Contrastingly, the dormant neurons we investigate here emerge over time and exacerbate with more gradient updates. In the interest of developing sample-efficient agents, scaling the replay ratio might require recycling the unused and dormant capacity. Similarly to the findings of Graesser et al. [2022], this work suggests there are important gains to be had by investigating the network architectures and topologies used for deep reinforcement learning.

Societal impact Although the work presented here is mostly of an academic nature, it aids in the development of more capable autonomous agents. While our contributions do not directly contribute to any negative societal impacts, we urge the community to consider these when building on our research.

Acknowledgements The authors would like to thank Max Schwarzer, Karolina Dziugaite, Marc G. Bellemare, Johan S. Obando-Ceron, Laura Graesser, Sara Hooker and Evgenii Nikishin, as well as the rest of the Brain Montreal team for their feedback on this work.

References

- Rishabh Agarwal, Dale Schuurmans, and Mohammad Norouzi. An optimistic perspective on offline reinforcement learning. In *International Conference on Machine Learning*, pages 104–114. PMLR, 2020.
- Rishabh Agarwal, Max Schwarzer, Pablo Samuel Castro, Aaron C Courville, and Marc Bellemare. Deep reinforcement learning at the edge of the statistical precipice. Advances in neural information processing systems, 34:29304–29320, 2021.

- Ibrahim Alabdulmohsin, Hartmut Maennel, and Daniel Keysers. The impact of reinitialization on generalization in convolutional neural networks. arXiv preprint arXiv:2109.00267, 2021.
- João Guilherme Madeira Araújo, Johan Samir Obando Ceron, and Pablo Samuel Castro. Lifting the veil on hyper-parameters for value-based deep reinforcement learning. In *Deep RL Workshop NeurIPS 2021*, 2021. URL https://openreview.net/forum?id=Ws4v7nSqqb.
- Samin Yeasar Arnob, Riyasat Ohib, Sergey Plis, and Doina Precup. Single-shot pruning for offline reinforcement learning. arXiv preprint arXiv:2112.15579, 2021.
- Jordan Ash and Ryan P Adams. On warm-starting neural network training. Advances in Neural Information Processing Systems, 33:3884–3894, 2020.
- Marc G Bellemare, Yavar Naddaf, Joel Veness, and Michael Bowling. The arcade learning environment: An evaluation platform for general agents. *Journal* of Artificial Intelligence Research, 47:253–279, 2013.
- Marc G Bellemare, Salvatore Candido, Pablo Samuel Castro, Jun Gong, Marlos C Machado, Subhodeep Moitra, Sameera S Ponda, and Ziyu Wang. Autonomous navigation of stratospheric balloons using reinforcement learning. *Nature*, 588(7836):77–82, 2020.
- Bruno Benedetti and Sebastien Couillard-Despres. Why would the brain need dormant neuronal precursors? *Frontiers in Neuroscience*, 16, 2022.
- Bruno Benedetti, Dominik Dannehl, Richard König, Simona Coviello, Christina Kreutzer, Pia Zaunmair, Dominika Jakubecova, Thomas M Weiger, Ludwig Aigner, Juan Nacher, et al. Functional integration of neuronal precursors in the adult murine piriform cortex. *Cerebral cortex*, 30(3):1499–1515, 2020.
- Emmanuel Bengio, Joelle Pineau, and Doina Precup. Interference and generalization in temporal difference learning. In *International Conference on Machine Learning*, pages 767–777. PMLR, 2020.
- Tudor Berariu, Wojciech Czarnecki, Soham De, Jörg Bornschein, Samuel L. Smith, Razvan Pascanu, and Claudia Clopath. A study on the plasticity of neural networks. *CoRR*, abs/2106.00042, 2021. URL https://arxiv.org/abs/2106.00042.
- Pablo Samuel Castro, Subhodeep Moitra, Carles Gelada, Saurabh Kumar, and Marc G. Bellemare.

- Dopamine: A Research Framework for Deep Reinforcement Learning. 2018. URL http://arxiv.org/abs/1812.06110.
- Xinyue Chen, Che Wang, Zijian Zhou, and Keith W Ross. Randomized ensembled double q-learning: Learning fast without a model. In *International Conference on Learning Representations*, 2020.
- Xiaoliang Dai, Hongxu Yin, and Niraj K Jha. Nest: A neural network synthesis tool based on a grow-andprune paradigm. *IEEE Transactions on Computers*, 68(10):1487–1497, 2019.
- Shibhansh Dohare, A Rupam Mahmood, and Richard S Sutton. Continual backprop: Stochastic gradient descent with persistent randomness. arXiv preprint arXiv:2108.06325, 2021.
- Lasse Espeholt, Hubert Soyer, Remi Munos, Karen Simonyan, Vlad Mnih, Tom Ward, Yotam Doron, Vlad Firoiu, Tim Harley, Iain Dunning, et al. Impala: Scalable distributed deep-rl with importance weighted actor-learner architectures. In *International conference on machine learning*, pages 1407–1416. PMLR, 2018.
- Utku Evci, Bart van Merrienboer, Thomas Unterthiner, Fabian Pedregosa, and Max Vladymyrov. Gradmax: Growing neural networks using gradient information. In *International Conference on Learning Representations*, 2021.
- Linxi Fan, Guanzhi Wang, De-An Huang, Zhiding Yu, Li Fei-Fei, Yuke Zhu, and Animashree Anandkumar. Secant: Self-expert cloning for zero-shot generalization of visual policies. In *International Conference on Machine Learning*, pages 3088–3099. PMLR, 2021.
- William Fedus, Prajit Ramachandran, Rishabh Agarwal, Yoshua Bengio, Hugo Larochelle, Mark Rowland, and Will Dabney. Revisiting fundamentals of experience replay. In *International Conference on Machine Learning*, pages 3061–3071. PMLR, 2020.
- Justin Fu, Aviral Kumar, Matthew Soh, and Sergey Levine. Diagnosing bottlenecks in deep q-learning algorithms. In *International Conference on Machine Learning*, pages 2021–2030. PMLR, 2019.
- Laura Graesser, Utku Evci, Erich Elsen, and Pablo Samuel Castro. The state of sparse training in deep reinforcement learning. In *International Conference on Machine Learning*, pages 7766–7792. PMLR, 2022.

- Sergio Guadarrama, Anoop Korattikara, Oscar Ramirez, Pablo Castro, Ethan Holly, Sam Fishman, Ke Wang, Ekaterina Gonina, Neal Wu, Efi Kokiopoulou, Luciano Sbaiz, Jamie Smith, Gábor Bartók, Jesse Berent, Chris Harris, Vincent Vanhoucke, and Eugene Brevdo. TF-Agents: A library for reinforcement learning in tensorflow. https://github.com/tensorflow/agents, 2018. URL https://github.com/tensorflow/agents. [Online; accessed 25-June-2019].
- Caglar Gulcehre, Srivatsan Srinivasan, Jakub Sygnowski, Georg Ostrovski, Mehrdad Farajtabar, Matt Hoffman, Razvan Pascanu, and Arnaud Doucet. An empirical study of implicit regularization in deep offline rl. arXiv preprint arXiv:2207.02099, 2022.
- Tuomas Haarnoja, Aurick Zhou, Pieter Abbeel, and Sergey Levine. Soft actor-critic: Off-policy maximum entropy deep reinforcement learning with a stochastic actor. In *International conference on machine* learning, pages 1861–1870. PMLR, 2018.
- Nicklas Hansen, Hao Su, and Xiaolong Wang. Stabilizing deep q-learning with convnets and vision transformers under data augmentation. In M. Ranzato, A. Beygelzimer, Y. Dauphin, P.S. Liang, and J. Wortman Vaughan, editors, Advances in Neural Information Processing Systems, volume 34, pages 3680–3693. Curran Associates, Inc., 2021. URL https://proceedings.neurips.cc/paper/2021/file/1e0f65eb20acbfb27ee05ddc000b50ec-Paper.pdf.
- Matteo Hessel, Joseph Modayil, Hado Van Hasselt, Tom Schaul, Georg Ostrovski, Will Dabney, Dan Horgan, Bilal Piot, Mohammad Azar, and David Silver. Rainbow: Combining improvements in deep reinforcement learning. In *Thirty-second AAAI conference on artificial intelligence*, 2018.
- Joel Hestness, Sharan Narang, Newsha Ardalani, Gregory Diamos, Heewoo Jun, Hassan Kianinejad, Md Patwary, Mostofa Ali, Yang Yang, and Yanqi Zhou. Deep learning scaling is predictable, empirically. arXiv preprint arXiv:1712.00409, 2017.
- Takuya Hiraoka, Takahisa Imagawa, Taisei Hashimoto, Takashi Onishi, and Yoshimasa Tsuruoka. Dropout q-functions for doubly efficient reinforcement learning. In *International Conference on Learning Representations*, 2021.
- Maximilian Igl, Gregory Farquhar, Jelena Luketina, Wendelin Boehmer, and Shimon Whiteson. Transient non-stationarity and generalisation in deep re-

- inforcement learning. In *International Conference* on Learning Representations, 2020.
- Michael Janner, Justin Fu, Marvin Zhang, and Sergey Levine. When to trust your model: Model-based policy optimization. Advances in Neural Information Processing Systems, 32, 2019.
- Łukasz Kaiser, Mohammad Babaeizadeh, Piotr Miłos, Błażej Osiński, Roy H Campbell, Konrad Czechowski, Dumitru Erhan, Chelsea Finn, Piotr Kozakowski, Sergey Levine, et al. Model based reinforcement learning for atari. In *International Conference on Learning Representations*, 2019.
- Jared Kaplan, Sam McCandlish, Tom Henighan, Tom B Brown, Benjamin Chess, Rewon Child, Scott Gray, Alec Radford, Jeffrey Wu, and Dario Amodei. Scaling laws for neural language models. arXiv preprint arXiv:2001.08361, 2020.
- Diederik P. Kingma and Jimmy Ba. Adam: A method for stochastic optimization. In Yoshua Bengio and Yann LeCun, editors, 3rd International Conference on Learning Representations, ICLR 2015, San Diego, CA, USA, May 7-9, 2015, Conference Track Proceedings, 2015. URL http://arxiv.org/abs/1412.6980.
- Robert Kirk, Amy Zhang, Edward Grefenstette, and Tim Rocktäschel. A survey of generalisation in deep reinforcement learning. arXiv preprint arXiv:2111.09794, 2021.
- Alex Krizhevsky, Geoffrey Hinton, et al. Learning multiple layers of features from tiny images. 2009.
- Aviral Kumar, Rishabh Agarwal, Dibya Ghosh, and Sergey Levine. Implicit under-parameterization inhibits data-efficient deep reinforcement learning. In International Conference on Learning Representations, 2021a.
- Aviral Kumar, Rishabh Agarwal, Tengyu Ma, Aaron Courville, George Tucker, and Sergey Levine. Dr3: Value-based deep reinforcement learning requires explicit regularization. In *International Conference on Learning Representations*, 2021b.
- Xingjian Li, Haoyi Xiong, Haozhe An, Cheng-Zhong Xu, and Dejing Dou. Rifle: Backpropagation in depth for deep transfer learning through re-initializing the fully-connected layer. In *International Conference on Machine Learning*, pages 6010–6019. PMLR, 2020.
- Timothy P Lillicrap, Jonathan J Hunt, Alexander Pritzel, Nicolas Heess, Tom Erez, Yuval Tassa, David Silver, and Daan Wierstra. Continuous control with deep reinforcement learning. In *ICLR* (*Poster*), 2016.

- Long-Ji Lin. Self-improving reactive agents based on reinforcement learning, planning and teaching. *Machine learning*, 8(3):293–321, 1992.
- Clare Lyle, Mark Rowland, and Will Dabney. Understanding and preventing capacity loss in reinforcement learning. In *International Conference on Learning Representations*, 2021.
- Volodymyr Mnih, Koray Kavukcuoglu, David Silver, Andrei A Rusu, Joel Veness, Marc G Bellemare, Alex Graves, Martin Riedmiller, Andreas K Fidjeland, Georg Ostrovski, et al. Human-level control through deep reinforcement learning. *nature*, 518(7540):529–533, 2015.
- Evgenii Nikishin, Max Schwarzer, Pierluca D'Oro, Pierre-Luc Bacon, and Aaron Courville. The primacy bias in deep reinforcement learning. In *International Conference on Machine Learning*, pages 16828–16847. PMLR, 2022.
- Martin L Puterman. Markov decision processes: discrete stochastic dynamic programming. John Wiley & Sons, 2014.
- Peter Rotheneichner, Maria Belles, Bruno Benedetti, Richard König, Dominik Dannehl, Christina Kreutzer, Pia Zaunmair, Maren Engelhardt, Ludwig Aigner, Juan Nacher, et al. Cellular plasticity in the adult murine piriform cortex: continuous maturation of dormant precursors into excitatory neurons. Cerebral Cortex, 28(7):2610–2621, 2018.
- Karthik Abinav Sankararaman, Soham De, Zheng Xu, W Ronny Huang, and Tom Goldstein. The impact of neural network overparameterization on gradient confusion and stochastic gradient descent. In *International conference on machine learning*, pages 8469–8479. PMLR, 2020.
- David Silver, Aja Huang, Chris J Maddison, Arthur Guez, Laurent Sifre, George Van Den Driessche, Julian Schrittwieser, Ioannis Antonoglou, Veda Panneershelvam, Marc Lanctot, et al. Mastering the game of go with deep neural networks and tree search. nature, 529(7587):484–489, 2016.
- Ghada Sokar, Elena Mocanu, Decebal Constantin Mocanu, Mykola Pechenizkiy, and Peter Stone. Dynamic sparse training for deep reinforcement learning. In *International Joint Conference on Artificial Intelligence*, 2022.
- Richard S Sutton. Learning to predict by the methods of temporal differences. *Machine learning*, 3(1):9–44, 1988.

- Richard S Sutton and Andrew G Barto. Reinforcement learning: An introduction. MIT press, 2018.
- Ahmed Taha, Abhinav Shrivastava, and Larry S Davis. Knowledge evolution in neural networks. In *Proceedings of the IEEE/CVF Conference on Computer Vision and Pattern Recognition*, pages 12843–12852, 2021.
- Yiqin Tan, Pihe Hu, Ling Pan, and Longbo Huang. Rlx2: Training a sparse deep reinforcement learning model from scratch. arXiv preprint arXiv:2205.15043, 2022.
- Emanuel Todorov, Tom Erez, and Yuval Tassa. Mujoco: A physics engine for model-based control. In 2012 IEEE/RSJ international conference on intelligent robots and systems, pages 5026–5033. IEEE, 2012.
- Hado van Hasselt, Yotam Doron, Florian Strub, Matteo Hessel, Nicolas Sonnerat, and Joseph Modayil. Deep reinforcement learning and the deadly triad. *CoRR*, abs/1812.02648, 2018. URL http://arxiv.org/abs/1812.02648.
- Hado P Van Hasselt, Matteo Hessel, and John Aslanides. When to use parametric models in reinforcement learning? Advances in Neural Information Processing Systems, 32, 2019.
- Kaixin Wang, Bingyi Kang, Jie Shao, and Jiashi Feng. Improving generalization in reinforcement learning with mixture regularization. In H. Larochelle, M. Ranzato, R. Hadsell, M.F. Balcan, and H. Lin, editors, Advances in Neural Information Processing Systems, volume 33, pages 7968-7978. Curran Associates, Inc., 2020. URL https://proceedings.neurips.cc/paper/2020/file/5a751d6a0b6ef05cfe51b86e5d1458e6-Paper.pdf.
- Lemeng Wu, Dilin Wang, and Qiang Liu. Splitting steepest descent for growing neural architectures. Advances in neural information processing systems, 32, 2019.
- Denis Yarats, Ilya Kostrikov, and Rob Fergus. Image augmentation is all you need: Regularizing deep reinforcement learning from pixels. In *International Conference on Learning Representations*, 2021. URL https://openreview.net/forum?id=GY6-6sTvGaf.
- Jaehong Yoon, Eunho Yang, Jeongtae Lee, and Sung Ju Hwang. Lifelong learning with dynamically expandable networks. In *International Conference on Learn*ing Representations, 2018.

- Sheheryar Zaidi, Tudor Berariu, Hyunjik Kim, Jörg Bornschein, Claudia Clopath, Yee Whye Teh, and Razvan Pascanu. When does re-initialization work? arXiv preprint arXiv:2206.10011, 2022.
- Xiaohua Zhai, Alexander Kolesnikov, Neil Houlsby, and Lucas Beyer. Scaling vision transformers. In *Proceedings of the IEEE/CVF Conference on Computer Vision and Pattern Recognition*, pages 12104–12113, 2022.
- Guanyu Zhou, Kihyuk Sohn, and Honglak Lee. Online incremental feature learning with denoising autoencoders. In *Artificial intelligence and statistics*, pages 1453–1461. PMLR, 2012.
- Hattie Zhou, Ankit Vani, Hugo Larochelle, and Aaron Courville. Fortuitous forgetting in connectionist networks. In *International Conference on Learning Representations*, 2021.

Table 1: Common Hyper-parameters for DQN and $DrQ(\epsilon)$.

Parameter	Value
Optimizer	Adam Kingma and Ba [2015]
Optimizer: ϵ	1.5×10^{-4}
Training ϵ	0.01
Evaluation ϵ	0.001
Discount factor	0.99
Replay buffer size	10^{6}
Minibatch size	32
Q network: channels	32, 64, 64
Q-network: filter size	$8 \times 8, 4 \times 4, 3 \times 3$
Q-network: stride	4, 2, 1
Q-network: hidden units	512
Recycling period	1000
au-Dormant	0.025 for default setting, 0.1 otherwise
Minibatch size for estimating neurons score	64

Table 2: Hyper-parameters for DQN.

Parameter	Value
Optimizer: Learning rate	6.25×10^{-5}
Initial collect steps	20000
n-step	1
Training iterations	Default setting: 40, otherwise: 10
Training environment steps per iteration	$250\mathrm{K}$
(Updates per environment step, Target network update period)	(0.25, 8000)
	(0.5, 4000)
	(1, 2000)
	(2, 1000)

A Experimental Details

Discrete control tasks. We evaluate DQN Mnih et al. [2015] on 17 games from the Arcade Learning Environment Bellemare et al. [2013]: Asterix, Demon Attack, Seaquest, Wizard of Wor, Bream Reader, Road Runner, James bond, Qbert, Breakout, Enduro, Space Invaders, Pong, Zaxxon, Yars' Revenge, Ms. Pacman, Double Dunk, Ice Hockey. This set is used by previous works Kumar et al. [2021a,b] to study the *implicit under-parameterization* phenomenon in offline RL. For hyper-parameter tuning, we used five games (Asterix, Demon Attack, Seaquest, Breakout, Beam Rider). We evaluate $DrQ(\epsilon)$ on the 26 games of Atari 100K Kaiser et al. [2019]. We used the best hyper-parameters found for DQN in training $DrQ(\epsilon)$.

Continuous control tasks. We evaluate SAC Haarnoja et al. [2018] on four environments from MuJoCo suite Todorov et al. [2012]: HalfCheetah-v2, Hopper-v2, Walker2d-v2, Ant-v2.

Code. For discrete control tasks, we build on the implementation of DQN and DrQ provided in Dopamine Castro et al. [2018] including the architectures used for agents. The hyper-parameters are provided in Tables 1, 2, and 3. For continuous control, we build on the SAC implementation in TF-Agents Guadarrama et al. [2018] and codebase of Graesser et al. [2022]. The hyper-parameters are provided in Table 4.

Evaluation. We follow the recommendation from Agarwal et al. [2021] to report reliable aggregated results across games using the interquartile mean (IQM). IQM is the calculated mean after discarding the bottom and top 25% of normalized scores aggregated from multiple runs and games.

Baselines. For weight decay, we searched over the grid $[10^{-6}, 10^{-5}, 10^{-4}, 10^{-3}]$. The best found value is 10^{-5} .

Table 3: Hyper-parameters for $DrQ(\epsilon)$.

Parameter	Value
Optimizer: Learning rate	1×10^{-4}
Initial collect steps	1600
<i>n</i> -step	10
Training iterations	40
Training environment steps per iteration	10K
Updates per environment step	1, 2, 4, 8

Table 4: Hyper-parameters for SAC.

Parameter	Value
Initial collect steps	10000
Discount factor	0.99
Training environment steps	10^{6}
Replay buffer size	10^{6}
Updates per environment step (Replay Ratio)	1, 2, 4, 8
Target network update period	1
target smoothing coefficient τ	0.005
Optimizer	Adam Kingma and Ba [2015]
Optimizer: Learning rate	3×10^{-4}
Minibatch size	256
Actor/Critic: Hidden layers	2
Actor/Critic: Hidden units	256
Recycling period	200000
au-Dormant	0
Minibatch size for estimating neurons score	256

For reset Nikishin et al. [2022], we consider re-initializing the last layer for Atari games (same as the original paper). They use a reset period of 2×10^4 in for Atari 100k Kaiser et al. [2019], which corresponds to having 5 restarts in a training run. Since we run longer experiments, we searched over the grid $[5 \times 10^4, 1 \times 10^5, 2.5 \times 10^5, 5 \times 10^5]$ gradient steps for reset period which corresponds to having 50, 25, 10 and 5 restarts per training (10M frames, replay ratio 1). The best found period is 1×10^5 . For SAC, we reset agent's networks entirely every 2×10^5 environment steps, following the original paper.

Replay ratio. For DQN, we evaluate replay ratio values: $\{0.25 \text{ (default)}, 0.5, 1, 2\}$. Following Van Hasselt et al. [2019], we scale the target update period based on the value of the replay ratio as shown in Table 2. For $DrQ(\epsilon)$, we evaluate the values: $\{1 \text{ (default)}, 2, 4, 8\}$.

ReDo hyper-parameters. We did the hyper-parameter search for DQN trained with RR = 1 using the nature CNN architecture. We searched over the grids [1000, 10000, 100000] and [0, 0.01, 0.1] for the recycling period and τ -dormant, respectively. We apply the best values found to all other settings of DQN, including the ResNet architecture, and $DrQ(\epsilon)$ as reported in Table 1.

Dormant neurons in supervised learning. Here we provide the experimental details of the supervised learning analysis illustrated in Section 3. We train a convolutional neural network on CIFAR-10 using stochastic gradient descent and cross entropy loss. We select 10000 samples from the dataset to reduce the computational cost. We analyze the dormant neurons in two supervised learning settings: (1) training a network with *fixed targets*, the standard single task supervised learning, where we train a network using the inputs and labels of CIFAR-10 for 100 epochs, and (2) training a network with *non-stationary targets*, where we shuffle the labels every 20 epochs to generate new targets. Table 5 provides the details of the network architecture and training hyper-parameters.

Table 5: Hyperparameters for CIFAR-10.

Parameter	Value
Optimizer	SGD
Minibatch size	256
Learning rate	0.01
Momentum	0.9
Architecture:	
Layer	(channels, kernel size, stride)
Convolution	(32, 3, 1)
Convolution	(64, 3, 1)
MaxPool	(-, 2, 2)
Convolution	(64, 3, 1)
MaxPool	(-, 2, 2)
Dense	(128, -, -)

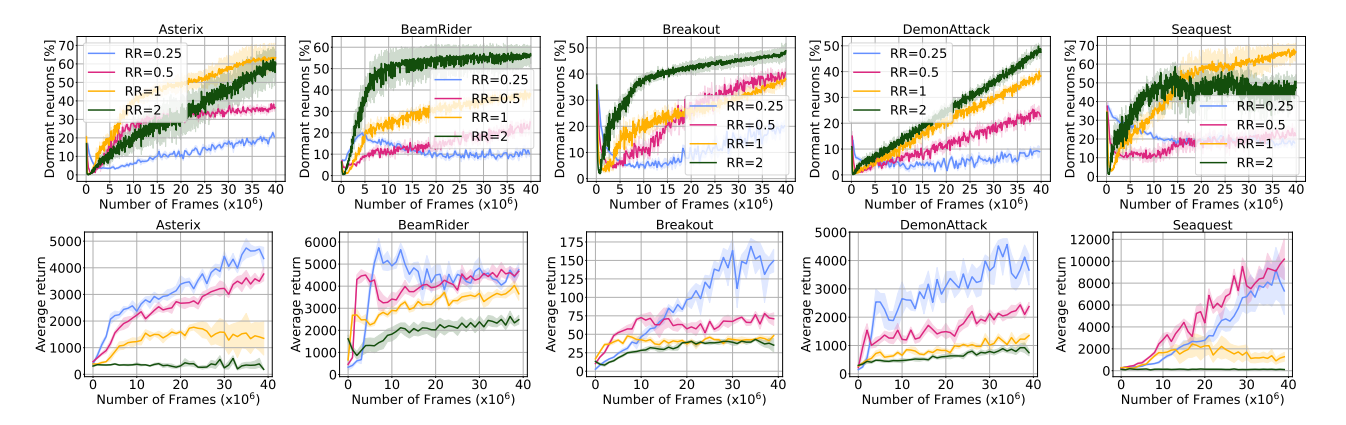


Figure 16: Effect of replay ratio in the number of dormant neurons for DQN on other Atari environments (experiments presented in Figure 7).

Learning ability of networks with dormant neurons. Here we present the details of the regression experiment provided in Section 3. Inputs and targets for regression come from a DQN agent trained on DemonAttack for 40M frames with the default hyper-parameters. The pre-trained network was trained for 40M frames using a replay ratio of 1.

B The Dormant Neuron Phenomenon in Different Domains

In this appendix, we demonstrate the dormant neuron phenomenon on $DrQ(\epsilon)$ Yarats et al. [2021] on Atari 100 benchmark Kaiser et al. [2019] and present more games for DQN. Additionally, we show the phenomenon on continuous control tasks and analyze the role of dormant neurons in performance. We consider SAC Haarnoja et al. [2018] trained on MuJoCo environments Todorov et al. [2012]. Same as our analyses in Section 3, we consider $\tau = 0$ to illustrate the phenomenon.

Figure 16 shows that across games, the number of dormant neurons consistently increases with higher values for the replay ratio in DQN. The increase in dormant neurons correlates with the performance drop observed in this regime. We then investigate the phenomenon on a modern valued-based algorithm $DrQ(\epsilon)$. As we see in Figure 17, the phenomenon emerges with increased number of training steps.

Figure 18 shows that the phenomenon is also present in continuous control tasks. An agent exhibits an increasing number of dormant neurons in the actor and critic networks in SAC. To analyze the effect of these

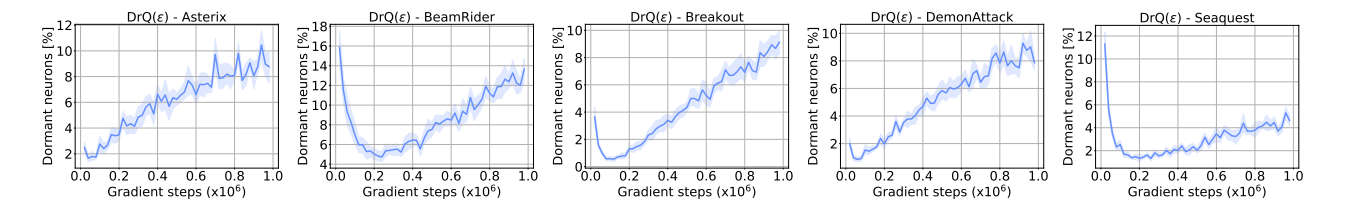


Figure 17: Dormant neuron phenomenon appears with increased number of training steps during the DrQ training.

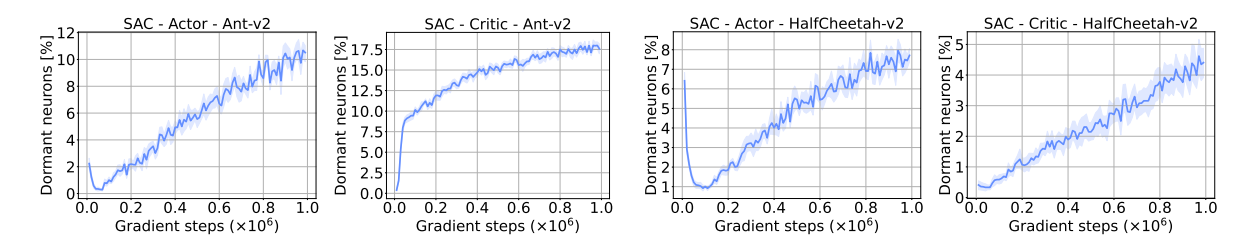


Figure 18: The number of dormant neurons increases over time during training SAC on MuJoCo environments.

neurons in performance, we prune dormant neurons every 200K steps. Figure 19 shows that the performance is not affected by pruning these neurons; indicating their little contribution to the learning process. Next we investigate the effect of ReDo and the studied baselines (Reset Nikishin et al. [2022] and weight decay) in this domain. Figure 20 shows that ReDo maintains the performance of the agents while other methods cause performance drop in most cases. We hypothesize that ReDo does not provide gains here as the state space is considerably low and the typically used network is sufficiently over-parameterized.

C Recycling Dormant Neurons

Here we study different strategies for growing dormant neurons and analyze the design choices of ReDo. We performed these analyses on DQN agents trained with RR = 1 and $\tau = 0.1$ on Atari games.

C.1 Effect of activation function

In this section we attempt to understand the effect of the activation function (ReLU) used in our experiments. ReLU activation function consists of a linear part (positive domain) with unit gradients and a constant zero part (negative domain) with zero gradients. Once the distribution of pre-activations fall completely into the negative part a neuron, it would stay there since the weights of the neuron would get zero gradients. This could be the explaination for increased number of dormant units in our neural networks. If this is the case, one might expect activations like leaky ReLU with non-zero gradients on the negative side to have significantly less dormant

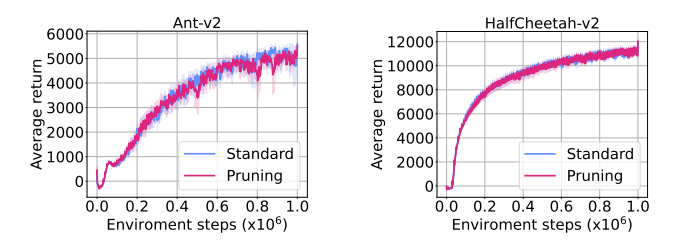


Figure 19: Pruning dormant neurons during training does not affect the performance of agents trained on MuJoCo environments.

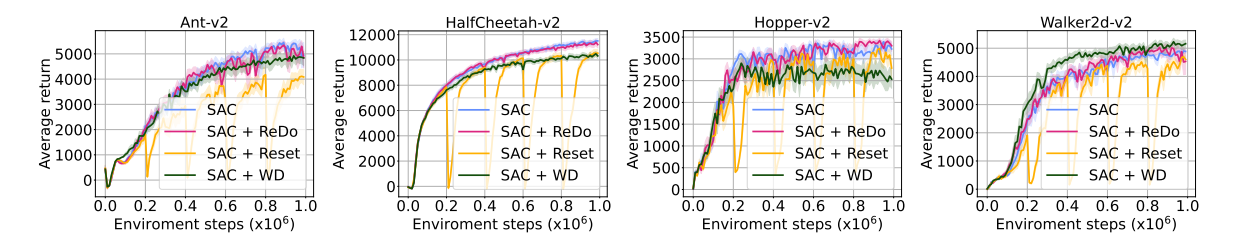


Figure 20: Comparison of the performance of SAC agents with ReDo and two different regularization methods.

neurons.

In Figure 21 we compare networks with leaky ReLU to original networks with ReLU activation. As we can see, using leaky ReLU slightly decreases the number of dormant neurons, but does not mitigate the issue. *ReDo* overcomes the performance drop occurs during training in the two cases.

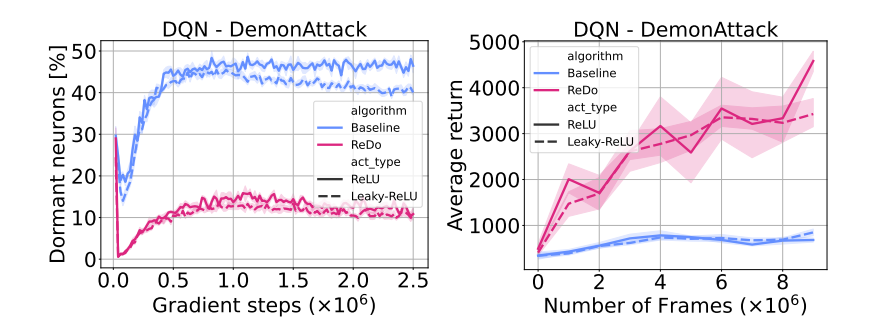


Figure 21: Training performance and dormant neuron characteristics of networks using leaky ReLU with negative slope of 0.01 (default value) compared to original networks with ReLU.

C.2 Recycling strategies

Outgoing connections. We investigate the effect of using random weights to reinitialize the outgoing connections of dormant neurons. We compare this strategy against the growing strategy of ReDo (zero weights). Figure 22 shows the performance of DQN on five examples of Atari games. The random initialization of the outgoing connections leads to a lower performance than the zero initialization. This is because the newly added random weights change the output of the network.

Incoming connections. Another possible strategy to grow the incoming connections is to scale their weights with the average norm of non-dormant neurons. We observe that this strategy has a similar performance to the random weight initialization strategy as shown in Figure 23.

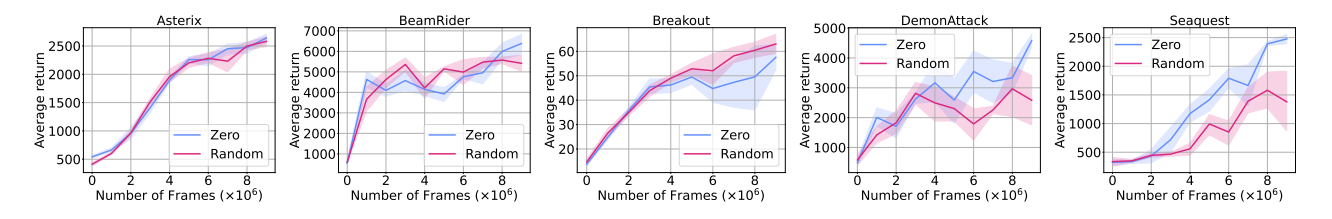


Figure 22: Comparison of performance with different strategies of reinitializing the outgoing connections of dormant neurons.



Figure 23: Comparison of performance with different strategies of reinitializing the incoming connections of dormant neurons.

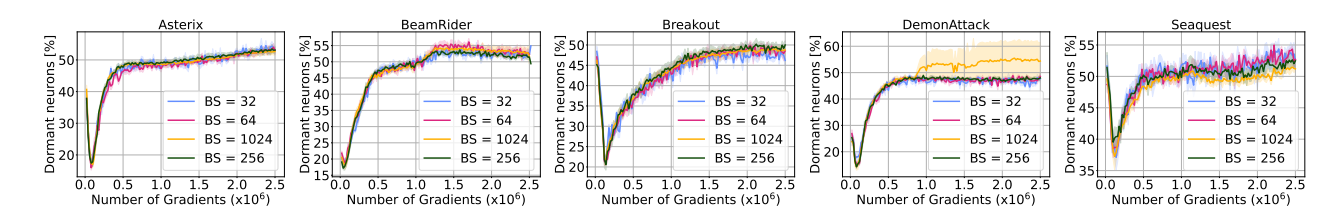


Figure 24: Effect of batch size used to detect dormant neurons.

C.3 Effect of batch size

The score of a neuron is calculated based on a given batch \mathcal{D} of data (Section 3). Here we study the effect of the batch size in determining the percentage of dormant neurons. We study four different values: $\{32, 64, 256, 1024\}$. Figure 24 shows that the identified percentage of dormant neurons are approximately the same using different batch sizes.

C.4 Comparison with Continual Backprop

Similar to experiments in Figure 15 we use a fixed recycling schedule to compare the activation based metric used by ReDo and the utility metric proposed by Continual Backprop [Dohare et al., 2021]. Results shown in Figure 25 show that both metrics achieve similar results. Note that the original Continual Backprop algorithm calculates neurons scores at every iteration and uses a running average to obtain a better estimates for the neuron saliency. This approach requires additional storage and compute compared to the fixed schedule used by our algorithm. Given the high dormancy threshold preferred by our method (i.e. more neurons are recycled), we expect better saliency estimates to have limited impact on the results presented here. However a more through analysis is needed to make general conclusions.

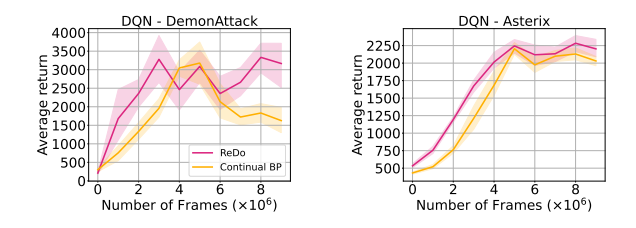


Figure 25: Comparison of different strategies for selecting the neurons that will be recycled.

D Performance Per Game

Here we share the results for each game for DQN (CNN) in the high replay ratio (RR=1) (Figure 26) and default setting (Figure 27).

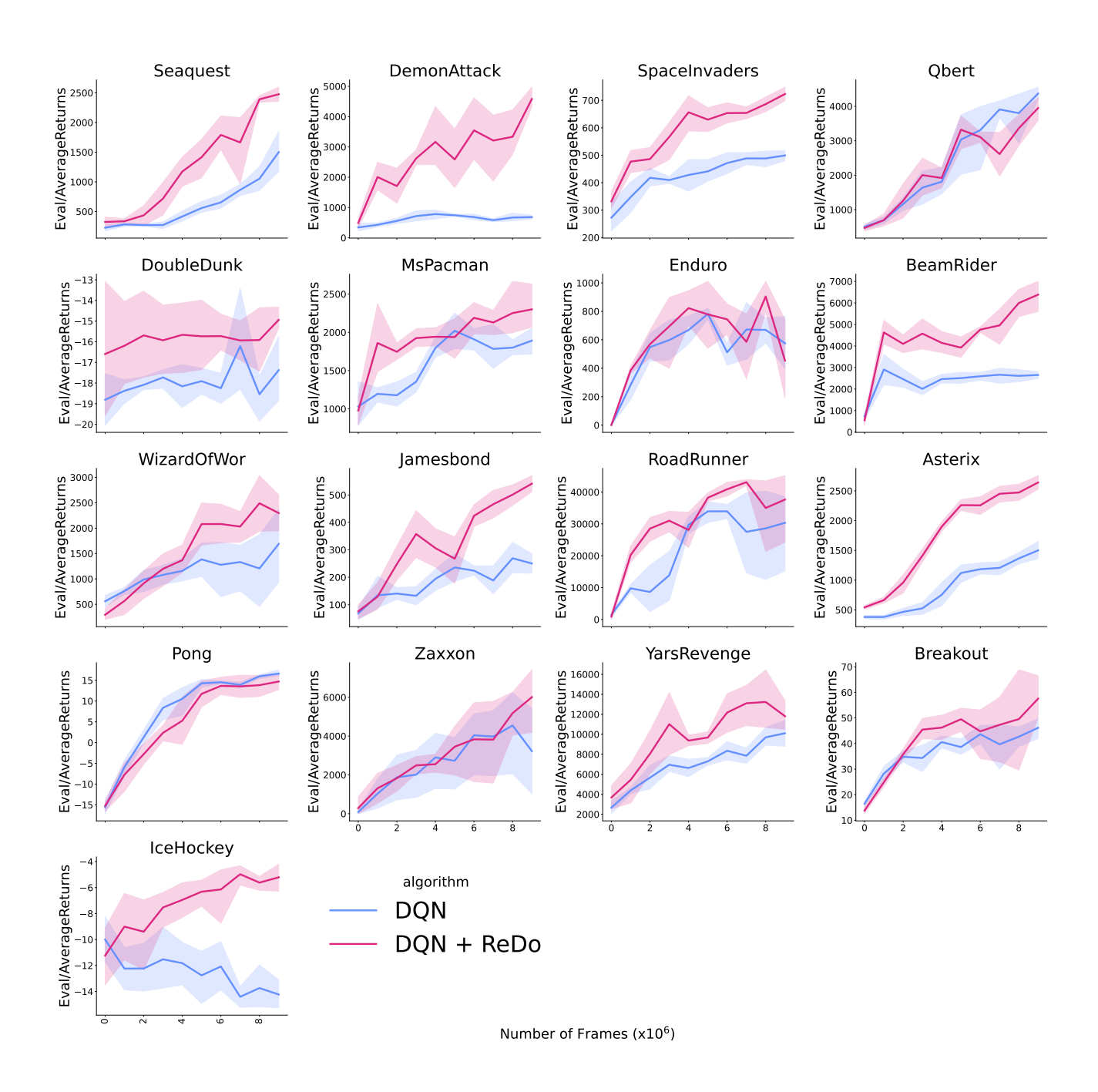


Figure 26: Training curves for DQN with the nature CNN architecture (Replay ratio=1).

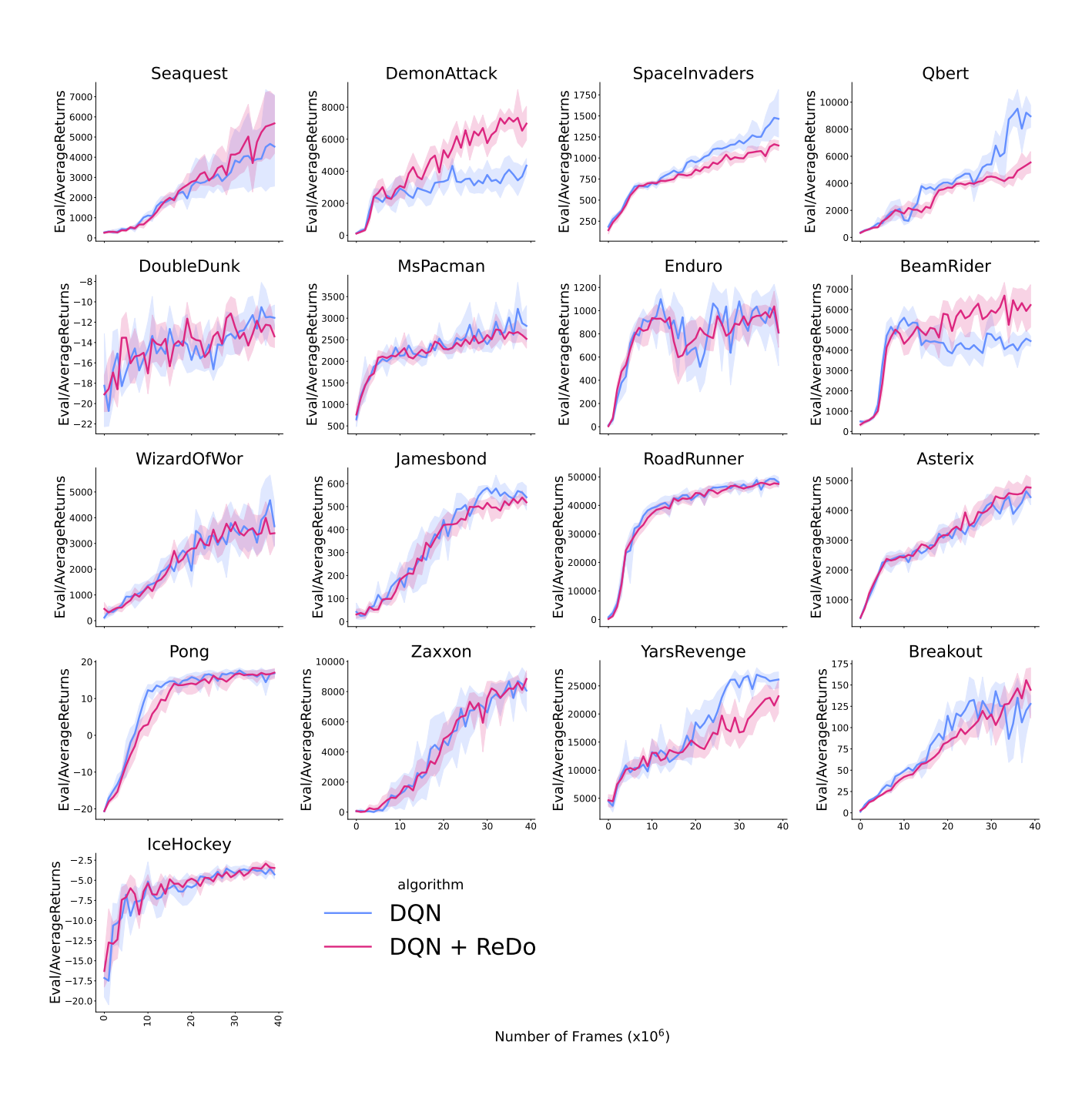


Figure 27: Training curves for DQN with the nature CNN architecture (Replay ratio=0.25).